

# Optimal Sizing of Substation-scale Energy Storage Station Considering Seasonal Variations in Wind Energy

Feng Zhang<sup>1</sup>, Zhao Xu<sup>2\*</sup>, Ke Meng<sup>3</sup>

<sup>1</sup> Key Laboratory of Power System Intelligent Dispatch and Control, Ministry of Education, Shandong University, Jinan, 250061, China

<sup>2</sup> Department of Electrical Engineering, The Hong Kong Polytechnic University, Hung Hom, Kowloon, Hong Kong SAR

<sup>3</sup> School of Electrical and Information Engineering, The University of Sydney, NSW, 2006, Australia

\* eezhaoxu@polyu.edu.hk

**Abstract:** This paper investigates an optimal sizing strategy for substation-scale energy storage station (ESS) that is installed at substations of transmission grids to provide services of both wind power fluctuation smoothing and power supply for peak load simultaneously. The proposed strategy firstly involves an optimal charging and discharging scheme enabling ESS to offer both services, considering particularly seasonal output variations of surrounding wind farms connected at the substation. Consequently, an optimization model of ESS capacity is formulated to achieve trade-off between various costs and benefits involved in offering services by ESS. Case studies based on historical wind power data are conducted to validate the performance of the proposed method, and the simulation results demonstrate that this method can significantly reduce the ESS size and achieve promising benefits from power supply for peak load.

## Nomenclature

$P_t^f$	fluctuation smoothing power
$P_t^s$	power for peak load
$P_t^{wind}$	wind power
$P_t^{ref}$	referenced wind power output
$t^{vi}, t^{vl}$	off-peak load period
$t^{pi}, t^{pl}$	peak load periods
$SOC_t$	SOC at time $t$
$V$	ESS rated energy capacity
$\Delta t$	data sampling interval
$SOC_t^0$	initial SOC of duration $t^{vi} \leq t < t^{vl}$
$SOC_t^1$	initial SOC of duration $t^{vl} \leq t < t^{pi}$
$SOC_t^2$	initial SOC of duration $t^{pi} \leq t \leq t^{pl}$
$SOC_t^3$	initial SOC of duration $t^{pl} \leq t < t^{vi}$
$P_{mc}$	maximum limits of charge power
$SOC_{max}$	maximum limits of SOC

$\eta^c$	charging efficiency
$\Delta P_t^{fc}$	charge power ramp of $P_t^f$
$\Delta P_t^{sc}$	charge power ramp of $P_t^s$
$P_{t-1}^f, P_{t-1}^s$	charge power values at the previous time step $t-1$
$\Delta P_{mc}$	maximum limit of charge power ramp
$P_{md}$	maximum limit of discharge power
$SOC_{min}$	minimum limit of SOC
$\Delta P_t^{fd}$	discharge power ramp of $P_t^f$
$\Delta P_t^{sd}$	discharge power ramp of $P_t^s$
$\Delta P_{md}$	maximum limit of discharge power ramp
$\eta^d$	discharging efficiency.
$Cyc_{remain}$	remaining life cycles
$Cyc_{rated}$	rated life cycles at certain DOD
$E_{used}$	total energy usage.
$N$	equivalent lifetime in year
$C^f$	fundamental cost
$\gamma$	construction cost per unit size
$\varepsilon$	installation cost per unit size
$inc$	annual interest rate
$C^p$	operation cost
$C^a$	cost due to the loss of wind power curtailment
$C^l$	penalty cost caused by the shortage of discharge power or energy reserve
$C^o$	penalty cost of overcharge or over-discharge
$SOC_H$	upper warning bounds of SOC
$SOC_L$	lower warning bounds of SOC
$T$	time duration of the data for sizing optimization
$[t_0, t_T]$	time interval of $T$
$\beta$	per unit cost of the curtailed wind energy
$\alpha$	per unit penalty cost of energy shortage for fluctuation smoothing.
$\theta$	per unit penalty cost of the overcharged or over-discharged energy
$F_i^{a-i} (i=1, 2, 3)$	Boolean functions to represent the conditions when wind power curtailment appears

$F_t^{l-i} (i=1, 2, 3)$	Boolean functions to show the energy or power shortage caused by the violation of $P_{md}$ , $SOC_{min}$ and $\Delta P_{md}$ respectively
$F_t^{o-i} (i=1, 2)$	Boolean functions to show the overcharged or over-discharged energy
$r^p, r^v$	electricity prices of peak and off-peak load period
$n$	equivalent days of period T
$S$	variance of wind power and referenced output
$k$	the number of time intervals during period T
$t_i^o, t_i^e$	initial and end moments of interval $i$ ( $1 < i \leq k$ )
$t_{rol}$	rolling operation step of ED
$M$	a positive integer
pdf	probability density function
cdf	cumulative distribution function
$P$	probability function
$P^c, P^d$	rated charge and discharge power
$P_t^{cw}$	curtailed wind power
$P_t^{sw}$	smoothed wind power.
$V_i (i=1, 2, 3)$	energy capacities determined in cases 1, 2 and 3
$V_4$	energy capacity in case 4
$E_y$	total energy of the three wind farms produced in one whole year

## 1. Introduction

Wind energy, one of the most popular renewable energy resources, has been widely deployed in recent years [1]. However, due to its stochastic nature, the increasing wind power penetration has imposed great challenge to the secure operation of power systems [2]. Along with the rise of wind penetration rate, power grids are experiencing difficulties in integrating more wind energy only with size-limited spinning reserve. In such a case, inevitably the wind power plants are required to constrain fluctuations of the power output, or they may face financial punishment. Therefore, countermeasures have to be developed to mitigate the wind power fluctuations [3].

The development of battery technologies provides an opportunity for mitigating wind fluctuations through ESS [4]. Distinguished from other technologies, ESS provides a fast and flexible solution to smoothing wind power fluctuations and increasing wind power penetration [5],[6]. Many researches have been directed towards the coordinated operation of wind-ESS recently. A dual-layer control strategy for

battery energy storage system was presented to mitigate wind power fluctuations in [7]. In [8], a control strategy was presented aiming at increasing renewable penetration while minimizing curtailment by energy buffering. A control strategy proposed in [9] took whole life span of storage system into account, considering operational constraints in the meanwhile. These studies mainly focus on controller design without considering the capacity of ESS. To make wind-ESS project more economically feasible, some studies focus on integrating wind farm with size-limited ESSs. From an economic perspective, when determining the capacity of ESS, there exists a trade-off between benefits and costs. Cost-benefit analysis of ESS has been conducted in previous works. In [10], the cost of flow-battery storage system was defined as a function of both power capacity and energy capacity. In [11], the cost of storage unit and power control unit accounts for the most of total system cost. In fact, a comprehensive economic analysis model should include not only the capital cost, such as battery management system (BMS), power control system (PCS), or battery pack, but also the operational cost, which is caused by wind power curtailment or unmet discharged or charged energy. Also, other factors can contribute to additional operational cost, e.g. over-charge/-discharge can damage the state-of-health (SOH) and significantly increase the operational cost. However, these factors are not included in most existing cost-benefit models. For instance, in [12] and [13], although either state-of-charge (SOC) or depth-of-discharge (DOD) had been constrained, additional costs due to SOC limits violations were not considered in assessing total operational cost.

Historical wind power generation data have been used to determine the size of ESS in [9]-[13]. However, wind power is a weather dependent power source, which shows clear seasonal patterns [14]. Generally, wind energy variations are volatile in high wind seasons, while the variability is small in mild wind seasons. Consequently, the optimal ESS sizing should consider the seasonal wind generation patterns and their impacts on ESS capacity utilizations [15]. For instance, fluctuations are smoothed with full ESS capacity in high wind seasons, while in mild wind seasons, ESS may operate at partial capacity. As such, with the spare energy capacity, ESS can potentially provide ancillary services such as power supply for peak load that generally receives higher incentives [16],[17]. If such benefits can be considered in ESS sizing process, more favourable investment plans can be obtained.

Given this background, in this paper, an optimal sizing strategy for substation-scale ESS is presented to achieve a better economic and technical performance. The main contributions of this paper include:

- 1) Seasonal variations of wind power generation is taken into consideration during the ESS sizing procedure, and the availability of power supply for peak load by spare ESS capacity is fully considered.

2) A novel ESS charge/discharge strategy is proposed in order to address the fluctuation smoothing for wind farm outputs and power supply for peak load simultaneously.

3) A comprehensive cost-benefit model is developed to facilitate ESS size optimization, where an operational cost model involving ancillary service benefits is introduced.

## 2. Preliminaries

Normally, pooling of a number of large-scale wind farms into clusters can provide several benefits. Due to smoothing effect of geography adjacent wind farms, the required size of substation-scale ESS can be reduced. Meanwhile, considering the seasonal wind variations, the spare ESS capacity can be used to provide ancillary service such as power supply for peak load to get extra benefits. Correspondingly charge/discharge control strategy for both fluctuation power smoothing and power supply for peak load is proposed.

### 2.1. ESS configuration

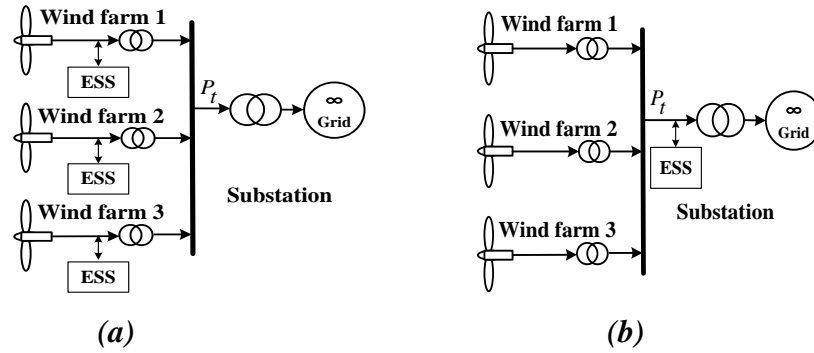


**Fig.1.** (a) ESSs installed at individual wind farm site in traditional configuration; (b) ESS installed at substation level for clustered wind farms

Since wind resources are greatly related to climate and geography conditions, wind farms are often built at areas with good wind resources, and several geography adjacent wind farms share one substation for grid integration. For power smoothing purposes, ESS is installed at individual wind farm site traditionally. However, as shown in Fig. 1(b), only one ESS is installed at substation site, which replaces dedicated ESSs equipped with each wind farm to avoid redundant investment in BMS, PCS, etc. Because of smoothing effect [18], the fluctuation of aggregated wind power at substation level can be mitigated [19]. Compared to the traditional configuration, the new topology can achieve similar power smoothing effect at lower cost and simpler structure. In terms of ESS ownership, there are two options, including wind farm ownership and utility ownership. Since the main objective of installing ESS is to smooth wind power fluctuation, it can be jointly-owned by multiple wind farms. Utility can also get involved in deploying ESS,

which can be dispatched to provide service to wind farms. However, despite ownership of ESS has a significant impact on business model, the ESS sizing methodology proposed in this paper still works.

## 2.2. Seasonal ESS Utilization and Power Supply for Peak Load

The seasonal wind variations could largely affect the ESS capacity utilization for power smoothing. The simulation results in [6] show that ESS utilization is apparently low with a steady SOC profile observed due to less variation in mild wind seasons especially in summer. Consequently, there exists a possibility of using spare ESS capacity to provide ancillary services.

Specifically, in traditional power grids with low wind penetration, thermal power plants still supply the majority of demand. Since the peak load power from ESS is not crucial and the focus of this research is to validate the feasibility of this additional service (power supply for peak load), ESS will adaptively supply the peak load power during certain peak and off-peak (low) load periods considering SOC conditions, and meanwhile the real-time load variation is not considered in this research. According to the actual load data in Shandong Province of China, Fig.2 shows the load curve of a typical working day. For simplicity, three different time periods are defined in this paper – peak (from 19:00 to 22:00), off-peak (from 03:00 to 06:00), and shoulder. Since electricity rate is a reflection of supply and demand, ESS can get extra benefits by shifting electricity generation from off-peak to peak periods on basis of time of use price. Other ancillary services, such as frequency regulation, are not considered since it may incur frequent charging or discharging for frequency control at any time that can affect its smoothing capability significantly.

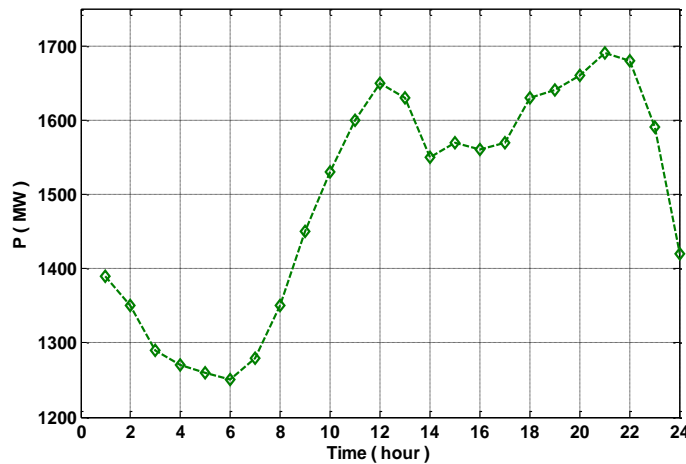


**Fig. 2.** Load curve of a typical working day

### 3. The charge/discharge control strategy for ESS

#### 3.1. Charging/discharging Strategy

The successful implementation of ESS relies heavily on operation strategy. Proper charging/discharging strategy can help ESS smooth wind power variations and shave peak demand simultaneously.

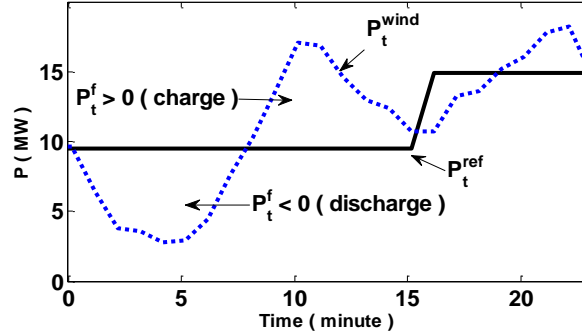


Fig. 3. Control rules of  $P_t^f$

To provide both power smoothing and power supply for peak load, the proposed ESS control strategy must be designed carefully. Fig. 3 and Table I illustrate the designed control logics of  $P_t^f$  and  $P_t^s$  respectively. As shown in Fig. 3,  $P_t^f$  is determined by both  $P_t^{wind}$  and  $P_t^{ref}$ . For comparison purposes, “positive” means charge, and “negative” denotes discharge. When  $P_t^{wind} > P_t^{ref}$ , the difference  $P_t^{wind} - P_t^{ref}$  is charged by  $P_t^f$ , and  $P_t^f > 0$  (charge), then  $P_t^{wind}$  can be smoothed to track  $P_t^{ref}$ . Otherwise,  $P_t^f$  has to release energy to fill the gap between  $P_t^{wind}$  and  $P_t^{ref}$ , and  $P_t^f < 0$  (discharge).

Table 1 Control logic rules of  $P_t^s$

Time period	$P_t^s$			
	$[t^{vi}, t^{vl}]$	$[t^{vl}, t^{pi}]$	$[t^{pi}, t^{pl}]$	$[t^{pl}, t^{vi}]$
	[03:00, 06:00]	[06:00, 19:00]	[19:00, 22:00]	[22:00, 03:00]
	Off-peak	Shoulder	Peak	Shoulder
State	Charge	---	Discharge	---
Power	$P_t^s \geq 0$	0	$P_t^s \leq 0$	0

In Table 1,  $t^{vi}$ ,  $t^{vl}$ ,  $t^{pi}$ ,  $t^{pl}$  vary as the region changes. In this paper,  $[t^{pi}, t^{pl}]$  and  $[t^{vi}, t^{vl}]$  are set as [19:00, 22:00] and [03:00, 06:00], respectively. From 03:00 to 06:00, ESS will be charged, and from 19:00 until 22:00, ESS will begin to discharge to meet the peak demand, and  $P_t^s \leq 0$ . Based on the control strategy of  $P_t^f$  and  $P_t^s$ , the SOC of each time step can be calculated as follows.

a) When  $t^{vi} \leq t < t^{vl}$  (power smoothing and energy store during off-peak load period)

$$SOC_t = SOC_{t^0} + \frac{1}{V} \cdot \sum_{t=t^{vi}}^{t^{vl}} P_t^f \cdot \Delta t \cdot \eta + \frac{1}{V} \cdot \sum_{t=t^{vi}}^{t^{vl}} P_t^s \cdot \Delta t \cdot \eta^c \quad (1)$$

Where  $\eta$  is the charging/discharging efficiency, and when  $P_t^f$  charges for fluctuation smoothing,  $\eta$  equals to  $\eta^c$ . Otherwise,  $\eta$  will be  $1/\eta^d$ .

b) When  $t^{vi} \leq t < t^{pi}$  (power smoothing only)

$$SOC_t = SOC_{t^1} + \frac{1}{V} \cdot \sum_{t=t^{vi}}^{t^{pi}} P_t^f \cdot \Delta t \cdot \eta \quad (2)$$

c) When  $t^{pi} \leq t \leq t^{pl}$  (power smoothing and energy release for peak load)

$$SOC_t = SOC_{t^2} + \frac{1}{V} \cdot \sum_{t=t^{pi}}^{t^{pl}} P_t^f \cdot \Delta t \cdot \eta + \frac{1}{V} \cdot \sum_{t=t^{pl}}^{t^{pi}} P_t^s \cdot \Delta t / \eta^d \quad (3)$$

d) When  $t^{pl} \leq t < t^{vi}$  (power smoothing only)

$$SOC_t = SOC_{t^3} + \frac{1}{V} \cdot \sum_{t=t^{pl}}^{t^{vi}} P_t^f \cdot \Delta t \cdot \eta \quad (4)$$

### 3.2. Referenced Wind Power Output

The referenced output shows the expected output after power smoothing by ESS. The deviation between the referenced output and wind power generation determines the charging/discharging power for ESS. Since during ESS planning, normally annual historical wind power data are used due to the periodic feature, the referenced output of annual wind power needs to be calculation first.

Under traditional schemes, the wind power is smoothed according to the referenced output curve on hourly basis to produce electricity [13]. Because of fixed time intervals, the referenced output curve can hardly track the variation feature of wind power. Meanwhile the reference output value is computed as the average wind power during time interval, and then much more energy needs to be charged or discharged to compensate the deviation between the wind generation and referenced output, which means higher power capacity and energy capacity of ESS would be required. On the contrary, if the time intervals are flexible to track the wind power feature, the capacity requirement of BESS can be greatly reduced. In this paper, with the aim to track the wind power better, the time intervals of referenced output are no longer fixed in order to best capture the wind variations and reduce the ESS capacity requirement.

Along with the increase of wind penetration, in order to guarantee the generation facilities to serve consumers reliably at the lowest cost, there is a trend for wind power to participate in the economic dispatch (ED) of power system. From the aspect of wind power control and dispatch, it is considered that the smoothed wind power can participate in ED of power system, as long as it satisfies the time interval requirement of rolling operation of ED. According to the rolling operation interval of ED, e.g., 10 minutes,



the time interval duration of referenced output can be  $M$  ( $M=1,2,3\dots$ ) times of the rolling operation interval of ED.

Subsequently, the presented referenced output aims to track the variation of wind power by minimizing the deviation between reference and wind power to reduce ESS capacity requirements. The reference output of annual historical wind power data is divided into  $k$  intervals and the corresponding time bounds are defined as  $(t_i^e, t_i^o]$  ( $i=1,2\dots k$ ). Notably, if  $k$  varies,  $P_t^{ref}$ ,  $t_i^e$  and  $t_i^o$  change as well. Hence, the referenced output in this research is determined as,

$$\text{Min } S = \sum_{i=1}^k \sum_{t=t_i^o}^{t_i^e} \left| \frac{P_t^{wind} - P_t^{ref}}{t_i^e - t_i^o} \right|^2 \quad (5)$$

According to the analysis of participation of ESS in rolling operation of ED, the duration of each time interval needs to meet the following requirements

$$t_i^e - t_i^o = M \cdot t_{rol} \quad (6)$$

Although the choice of  $t_{rol}$  varies in different power systems, the choice of  $t_{ro}$  will not affect the referenced power calculation. In this paper, the typical system dispatch interval is set as 10 minutes [20]. With this objective function,  $k$  and the  $P_t^{ref}$ ,  $t_i^o$  and  $t_i^e$  of each time interval can be calculated.

### 3.3. Wind Power Curtailment and Shortage of Discharge Power or Energy

Since ESS is limited in capacity, when ESS cannot store all the supposed energy, the surplus wind energy will be curtailed. Likewise, if ESS is short of discharge power or energy reserve, shortage of discharge power or energy may occur and results in the deficient smoothing.

1) *Wind Power Curtailment*: Three factors including the maximum charge power, SOC limit, and ramping rate, can result in wind power curtailment, which are expressed as

$$P_t^f + P_t^s > P_{mc}/\eta^c \quad (7)$$

$$SOC_t > SOC_{max} \quad (8)$$

$$\Delta P_t^{fc} + \Delta P_t^{sc} > \Delta P_{mc}/\eta^c \quad (9)$$

and

$$\Delta P_t^{fc} = P_t^f - P_{t-1}^f \quad (10)$$

$$\Delta P_t^{sc} = P_t^s - P_{t-1}^s \quad (11)$$

It can be seen that wind curtailment occurs when charge power, SOC, or charge power ramp exceeds the limits.

2) *Shortage of discharge power or energy*: Due to the maximum discharge power limits, discharge power ramp, and minimum SOC limit, ESS discharge power or energy can be limited, and the fluctuations cannot be smoothed effectively:

$$|P_t^f + P_t^s| > |P_{md}| \cdot \eta^d \quad (12)$$

$$SOC_t < SOC_{min} \quad (13)$$

$$|\Delta P_t^{fd}| + |\Delta P_t^{sd}| > |\Delta P_{md}| \cdot \eta^d \quad (14)$$

#### 4. Cost-benefit analysis of ESS

Economic performance is crucial in ESS planning. Based on the proposed charge/discharge strategy, a comprehensive cost-benefit model including fundamental cost and operational cost is built to determine the optimal ESS capacity, where benefits from power supply for peak load are considered.

##### 4.1. ESS Lifetime Model

The rated ESS lifetime is denoted as the life cycles within certain DOD, while the actual lifetime varies with the usage of ESS. In this research, the equivalent lifetime model is used to calculate the remaining charging/discharging capacity [21]. This method assesses the remaining life cycles of ESS according to the total energy usage. The remaining life cycle is calculated as

$$Cyc_{remain} = \frac{Cyc_{rated} DOD - E_{used}}{Cyc_{rated} DOD} Cyc_{rated} \quad (15)$$

Based on annual energy usage, the equivalent lifetime is calculated as

$$N = \frac{Cyc_{rated}}{Cyc_{rated} - Cyc_{remain}} \quad (16)$$

##### 4.2. Comprehensive Cost Model

1) *Fundamental Cost Model*: The fundamental cost  $C^f$  takes the time value of capital into consideration, and is expressed as

$$C^f = (\gamma + \varepsilon) \cdot V \cdot (1 + inc)^N \quad (17)$$

2) *Operation Cost Model*: the operation cost consists of three parts that are described as

$$C^p = C^a + C^l + C^o \quad (18)$$

As discussed in Section 2,  $C^a$  is the loss due to wind power curtailment, and  $C^l$  is the penalty cost caused by the shortage of discharge power or energy reserve.  $C^o$  is the penalty cost of overcharge or over-discharge so as to avoid severe damage to SOH of the ESS. Here when  $SOC_t$  crosses the warning limits

$SOC_H$  and  $SOC_L$ , ESS can keep charging until  $SOC_{max}$ , or discharging until  $SOC_{min}$ . However, the penalty cost has to be paid.

Specifically,  $C^a$  can be calculated in (19), and  $F_t^{a-i}$  ( $i=1, 2, 3$ ) are the Boolean functions to represent the conditions when wind power curtailment appears, as shown in (20).

$$C^a = \beta \cdot \left\{ \sum_{t=t_0}^{t_f} F_t^{a-1} \cdot \left( P_t^{wind} - P_t^{ref} + P_t^s - \frac{P_{mc}}{\eta^c} \right) \Delta t + \sum_{t=t_0}^{t_f} F_t^{a-2} \cdot \left[ \left( P_t^{wind} - P_t^{ref} + P_t^s \right) \Delta t - \frac{(SOC_{max} - SOC_{t-1})V}{\eta^c} \right] \right. \\ \left. + \sum_{t=t_0}^{t_f} F_t^{a-3} \cdot \left( \Delta P_t^f + \Delta P_t^s - \Delta P_{mc} / \eta^c \right) \Delta t \right\} \quad (19)$$

$$F_t^{a-i} = \begin{cases} 1 & \left( P_t^{wind} - P_t^{ref} + P_t^s - \frac{P_{mc}}{\eta^c} \right) > 0 \text{ \& } i=1 \\ 1 & SOC_t - SOC_{max} > 0 \text{ \& } i=2 \\ 1 & \left( \Delta P_t^f + \Delta P_t^s - \Delta P_{mc} / \eta^c \right) > 0 \text{ \& } i=3 \end{cases} \quad (20)$$

In (19),  $C^a$  is expressed as the sum of three parts in the braces. The first part shows curtailed wind energy which is caused when charge power violates the limitation, and  $F_t^{a-1}$  is its Boolean function to judge whether it occurs. Similarly, the second and third terms denote the curtailed wind energy caused by the violation of  $SOC_{max}$  and  $\Delta P_{mc}$  respectively, and the Boolean functions are tracked in  $F_t^{a-2}$  and  $F_t^{a-3}$ .

Likewise,  $C^l$  can be computed as follow.

$$C^l = \alpha \cdot \left\{ \sum_{t=t_0}^{t_f} F_t^{l-1} \cdot \left( | P_t^{wind} - P_t^{ref} + P_t^s - P_{md} \cdot \eta^d | \right) \Delta t + \sum_{t=t_0}^{t_f} F_t^{l-2} \cdot \left[ | P_t^{wind} - P_t^{ref} + P_t^s | \Delta t - (SOC_{t-1} - SOC_{min})V \cdot \eta^d \right] \right. \\ \left. + \sum_{t=t_0}^{t_f} F_t^{l-3} \cdot \left( | \Delta P_t^f + \Delta P_t^s - \Delta P_{md} \cdot \eta^d | \right) \Delta t \right\} \quad (21)$$

$C^l$  in (21) also consists of three parts, which show the energy or power shortage caused by the violation of  $P_{md}$ ,  $SOC_{min}$  and  $\Delta P_{md}$  respectively, and the Boolean functions  $F_t^{l-i}$  ( $i=1, 2, 3$ ) are defined as

$$F_t^{l-i} = \begin{cases} 1 & \left( P_t^{wind} - P_t^{ref} + P_t^s - P_{md} \cdot \eta^d \right) < 0 \text{ \& } i=1 \\ 1 & SOC_t - SOC_{min} < 0 \text{ \& } i=2 \\ 1 & \left( \Delta P_t^f + \Delta P_t^s - \Delta P_{md} \cdot \eta^d \right) > 0 \text{ \& } i=3 \end{cases} \quad (22)$$

Furthermore,  $C^o$  is calculated as

$$C^o = \theta \cdot \left\{ \sum_{t=t_0}^{t_f} F_t^{o-1} \cdot (SOC_t - SOC_H) \cdot V + \sum_{t=t_0}^{t_f} F_t^{o-2} \cdot |SOC_t - SOC_L| \cdot V \right\} \quad (23)$$

$F_t^{o-i}$  ( $i=1, 2$ ) are shown as

$$F_t^{o-i} = \begin{cases} 1 & (SOC_t - SOC_H) > 0 \& i = 1 \\ 1 & (SOC_t - SOC_L) < 0 \& i = 2 \end{cases} \quad (24)$$

3) *Benefits from Power Supply for Peak Load:* Based on the control logic rules of  $P_t^s$  in Table 1, the diurnal benefits from power supply for peak load can be calculated as,

$$B_d = \sum_{t=t^{pi}}^{t^{pl}} r^p \cdot |P_t^s| \cdot \Delta t \cdot \eta^d - \sum_{t=t^{vi}}^{t^{vl}} \frac{r^v \cdot P_t^s \cdot \Delta t}{\eta^c} \quad (25)$$

In Eq. (25), the first component represents the produced benefits from discharging ESS to serve demand during peak load period at price  $r^p$ , while the second component denotes the incurred cost for charging ESS during the off-peak period at price  $r^v$ .

The total benefits from power supply for peak load during period T can be calculated as the sum of diurnal benefits.

$$B_{total} = \sum_{i=1}^n B_d^i \quad (26)$$

## 5. Optimal sizing methodology

Based on the proposed charge/discharge strategy and the cost-benefit model, the ESS power capacity and energy capacity will be determined.

### 5.1. Energy Capacity Determination

To minimize the total investment, the proposed energy capacity optimization model considers the capital expenditures from construction to operation, and benefits from power supply for peak load. The objective function is expressed as

$$\text{Min } C = \frac{C^f}{N} + C^p - B_{total} \quad (27)$$

It should be noted that  $C^f$  and  $C^p$  are mutually coupled, which means if lower energy capacity is selected, operation conditions of ESS and the effectiveness of power smoothing cannot be guaranteed, also this brings about significant increase of  $C^p$ . However, the consideration of  $B_{total}$  equivalently decreases the  $C^p$ , thus it trends to reduce  $C^f$ , and the energy capacity requirement as well. Obviously, the determination of ESS energy capacity is the trade-off between  $C^f$  and  $C^p - B_{total}$ .

### 5.2. Power Capacity Determination

In this paper, the ESS power capacity is determined statistically with probability density function (pdf) of  $P_t^f$ . The rated power capacity  $P^c$  and  $P^d$  are expected to meet the charge and discharge power with the probability of  $p$  ( $0 < p \leq 1$ ). It can be observed that the rated power capacity strongly depends on the selection of  $p$ . If  $p$  is too small, there will be more charge/discharge power that are higher than the rated values, then more wind power will be curtailed, or more discharge power is short for effective smoothing. On the other side, if  $p$  is too large, the rated power will be increased accordingly to satisfy the charge/discharge requirements, which will increase the investment cost. For this reason, in order to get a reasonable power capacity, based on the previous work in [13],  $p$  is set as 0.95 in this study. The rated charge and discharge power can be determined by

$$P(0 \leq P_t^f \cdot \eta^c \leq P^c) = p \quad P_t^f > 0 \quad (28)$$

$$P(P^d \leq P_t^f / \eta^d \leq 0) = p \quad P_t^f < 0 \quad (29)$$

### 5.3. Procedures of the Proposed Optimal Sizing Methodology

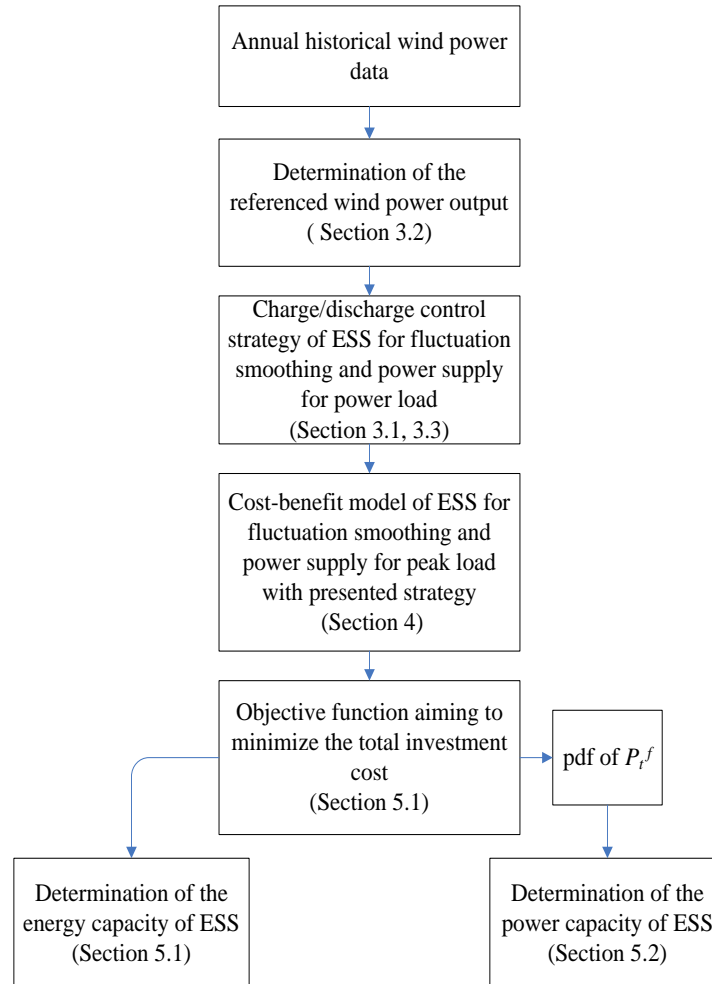


**Fig.4.** Procedures of the Optimal Sizing Methodology

The procedure of the optimal sizing methodology is presented to make it more legible, as shown in Fig.4. The ESS sizing methodology mainly includes the determination of both energy capacity and power capacity. Considering the annual period feature of wind power generation, annual historical wind power data is collected for ESS planning. To set up a specific power smoothing target, the determination of referenced wind output is presented. Afterwards, the charging/discharging control strategy of ESS considering the seasonal wind variations is proposed for power smoothing and power supply for peak load. According to the control strategy, the cost-benefit model of ESS is analysed for building the objective function for sizing the capacity of ESS. After the solution of objective function, the optimal energy capacity can be determined, and meanwhile the pdf of  $P_t^f$  can also be computed to determine the power capacity of ESS.

## 6. Case study

The presented sizing strategy is verified using wind generation data of three clustered wind farms located on the southeast coast of Shandong Province in China. The installed capacity of the wind farms are 45 MW, 39 MW, and 66 MW respectively. Lead-acid battery is selected in this paper for its excellent performance and low price [17], [22], and Table 2 shows the ESS operating parameters.

**Table 2** ESS operating parameters

$SOC_H$	$SOC_{min}$	$p$	$\Delta P_{mc}$	$\eta^c$	$C_{yCrated}$
0.85	0.1	0.95	9.6 MW	0.85	2500
$SOC_L$	$SOC_{max}$	$\Delta t$	$\Delta P_{md}$	$\eta^d$	T
0.2	1.0	5min	9.2 MW	0.9	1 year

The cost and price settings need to be reasonable as they are crucial for the sizing determination. The construction cost per unit size  $\gamma$  is assumed to be  $5.9 \times 10^5$  \$/MWh [22]. According to [22]-[25], the typical costs are shown in Table 3, and all the parameters are the per unit values of  $\gamma$  in electricity market.

**Table 3** Typical costs and prices

Fundamental cost			Operation cost ( $10^{-3}$ )			Electricity prices ( $10^{-3}$ )	
$\gamma$	$\varepsilon$ ( $10^{-3}$ )	$Inc$	$\beta$	$\alpha$	$\theta$	$r^p$	$r^v$
1.0	0.1	0.05	0.21	1.0	4.0	0.4	0.1

It should be noted that price ratio between  $r^p$  and  $r^v$  is 4, which is a common setting nowadays in electricity market with the aim to encourage power consumption during off peak period. Furthermore, as the highest price among the operation costs,  $\theta$  is 0.4% of the construction price  $\gamma$ , but ten times of  $r^p$ . The rea-

son is that frequent overcharge or over-discharge may severely damage ESS, greatly affecting the lifetime of ESS. Thus, as a penalty cost,  $\theta$  is set as a high value to limit overcharge or over-discharge.

### 6.1. ESS Power and Energy Capacity

1) *Power capacity*: The pdf of charge and discharge power are statistically quantified. Then, the cdf can be calculated. Fig. 5 shows the pdf and cdf curves of both charge and discharge power. When cdf equals  $p$ , the corresponding power can be defined as the rated power. As shown in Fig. 5, the rated charge power can be determined as 7.4 MW, while the rated discharge power is 7.1 MW. In addition, in order to limit over charge or over discharge power,  $P_{mc}$  is set equal to  $P^c$ , and in a similar way,  $P_{md}$  is the same as  $P^d$ .

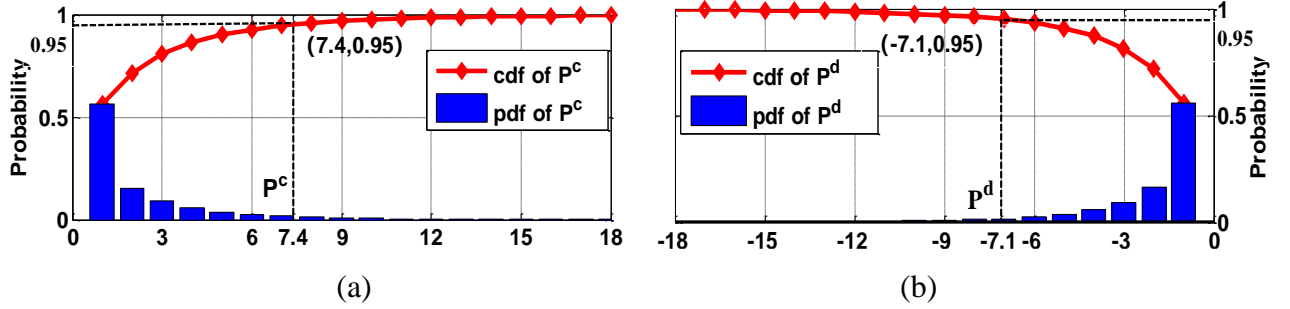


Fig.5. pdf and cdf curves of the charge and discharge power (MW)

2) *Energy capacity*: Table 4 presents the results of four case studies. It can be seen that the proposed strategy is studied in case 4, while different configurations with respect to ESS location, adoption of referenced output, and consideration seasonal variations are applied in other cases in order to assess the advantages of the proposed strategy through comparisons.

**Table 4** Operating strategy in various cases

ID	ESS at the substation	Referenced output	Wind seasonal variations
Case 1	Yes	Hourly constant output	Considered
Case 2	Yes	The proposed referenced output	Ignored
Case 3	No	The proposed referenced output	Considered
Case 4	Yes	The proposed referenced output	Considered

Specifically, in case 1, ESS is located at the substation to smooth the fluctuations on an hourly basis, and the control strategy considers the wind seasonal variation to earn benefits from power supply for peak load. So the comparison between cases 1 and 4 will verify whether the optimal referenced output proposed in this paper can decrease the energy capacity of ESS. Case 2 has the same ESS configuration and referenced output, but ignores the wind seasonal variations and the opportunity of earning benefits from power

supply for peak load. It will be compared with case 4 to verify whether the benefits from power supply for peak load have an ability of reducing energy capacity. Moreover, case 3 is used to show whether the ESS configuration plays a role in decreasing energy capacity.

Furthermore, to ensure the four cases are comparable, two performance indexes are proposed and are defined as follows.

*Ratio of curtailed energy to total energy produced  $E_c$* : During the ESS sizing procedure, there is curtailed wind power incurred by ESS operation.  $E_c$  is defined as the sum of the curtailed wind energy divided by total energy of the three wind farms produced in one year, aiming at assessing the effective utilization of wind resources.

$$E_c = \frac{1}{E_y} \cdot \sum_{t=t_0}^{t_r} P_t^{cw} \cdot \Delta t \quad (30)$$

*Deviation rate  $D_r$* :  $D_r$  is derived from the difference of the referenced output and the smoothed output to evaluate their smoothing effectiveness.  $D_r$  is used to assess whether the referenced output is perfectly tracked during the fluctuation smoothing.

$$D_r = \sum_{t=t_0}^{t_r} \left| \frac{P_t^{sw} - P_t^{ref}}{P_t^{ref}} \right| \cdot \Delta t \quad (31)$$

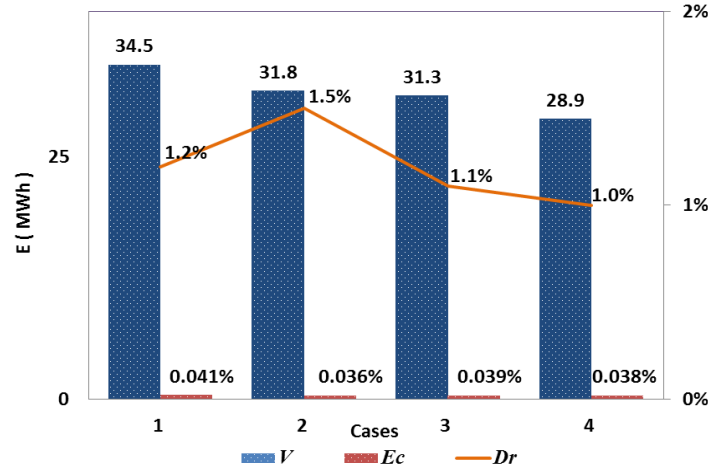


**Fig.6.** Simulation results of the energy capacity determination

Fig.6 shows the simulation results including evaluation parameters  $E_c$ ,  $D_r$  and energy capacity  $V$ . It can be observed that  $E_c$  of the four cases have small differences, and  $E_c$  in case 2 is the smallest because there is no power supply for peak load.  $D_r$  in all cases are also very close. These two parameters effectively assess the smoothing effectiveness by the storage. The ESS capacity is determined at 34.5 MWh in case 1, where the ESS smooths the fluctuations on an hourly basis. In contrast with the capacity of 28.9 MWh



determined in case 4, the strategy of case 1 needs 19.4% more capacity, which is due to the hourly reference used. In other words, the proposed strategy can decrease the energy capacity by 19.4% compared with the strategy using the hourly reference because of its optimal referenced power output of variable intervals. The energy capacity in case 2 is determined at 31.8 MWh, which implies that the benefits of power supply for peak load play a great role in the energy capacity reduction. Furthermore, because of dispersed ESSs in case 3, 8.3% more total stage capacity is needed compared with case 4, which justifies the smoothing effect of clustered wind farms and the installation of ESS at substation really play a part in mitigating the fluctuations and reducing ESS capacity requirement accordingly. Base on the analysis, it also should be noted that the proposed referenced output, participation into power supply for peak load and ESS installation at substation all contribute the effective energy capacity reduction for proposed strategy.

## 6.2. Fluctuation Smoothing

Two cases are selected to demonstrate the smoothing performance. Case 1 represents the mild wind season when the unutilized energy capacity can participate in power supply for peak load to achieve extra benefits. Case 2 shows the fluctuation smoothing in wild wind season when little or even none capacity participates in power supply for peak load because of the dramatic fluctuations.

1) *Case1*: In this case, wind power data of a typical day in July when the wind is mild with infrequent dramatic fluctuations is selected for demonstration. From Fig.7, it can be seen that the values of the smoothed wind power  $P_t^{sw}$  are almost identical with the referenced wind power  $P_t^{ref}$ , which means that  $P_t^{sw}$  shows a perfect performance in tracking  $P_t^{ref}$ .

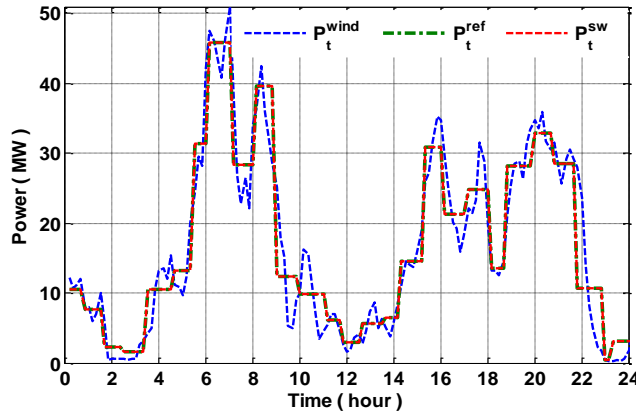


**Fig.7.** Smoothing effectiveness of a typical day in July

Besides, Fig. 8 shows the SOC curve without power supply for peak load and the SOC curve by the proposed control strategy. The SOC without power supply for peak load varies between 0.35 and 0.7,

which implies that partial ESS capacity is free to charge or discharge, which verifies that ESS can play a role in ancillary services in such seasons. From the SOC curve by the proposed control strategy, it can be observed that when participating in power supply for peak load, the ESS charges at off-peak load period, and then SOC reaches a higher but reasonable level, while during peak load period, ESS discharges for power supply for peak load resulting in a lower SOC level as well. However, it should be noted that the proposed optimization model can compute an available power for peak load, as shown in the bottom of Fig. 8, to achieve maximal benefits and keep SOC in a good condition, which means that the optimization model can well achieve the tradeoff between the benefits from power supply for peak load and the risk of an increase in operation cost caused by the participation in power supply for peak load.

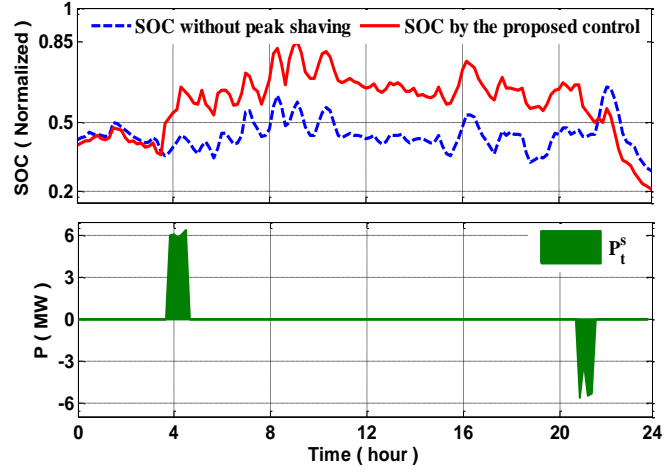


*Fig. 8. SOC and power supply for peak load of a typical day in July*

2) *Case 2:* In this case, wind power data of a typical day in December is chosen to illustrate the smoothing performance in wild wind season with dramatic fluctuations.

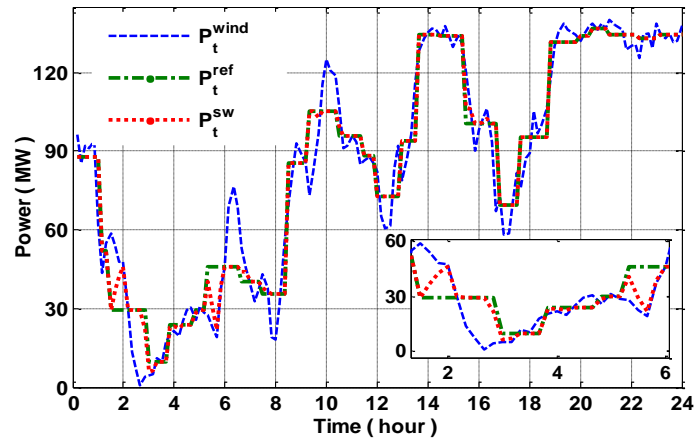


*Fig. 9. Smoothing effectiveness of a typical day in December*

In Fig. 9 it can be seen that ESS has difficulties in smoothing all the fluctuations. During some time sections where wind power varies dramatically, e.g. between 1:00 and 2:00, the size-limited ESS cannot charge all supposed energy, and subsequently  $P_t^{sw}$  cannot track  $P_t^{ref}$  effectively. During other sections, e.g. between 5:00 and 6:00, ESS is short of discharge energy, resulting in obvious deviation between  $P_t^{sw}$  and  $P_t^{ref}$ .

These scenarios imply that in winter, even all determined ESS capacity is arranged for fluctuation smoothing, the wind power still cannot be perfectly smoothed. The reason is that the determined energy capacity considers the trade-off of wind conditions in four seasons. So the seasonal feature of the wind power variations determines that the most severe fluctuations in winter need even higher capacity than the determined energy capacity. Consequently, according to the objective function for energy capacity determination, there is no doubt that ESS will quit the power supply for peak load in such season, but focus on the fluctuation smoothing.

### 6.3. Benefit Analysis of Power Supply for Peak Load

With the determination of ESS capacity, the daily capacity allocation and benefits of power supply for peak load can be calculated. Based on this, Table 5 provides the monthly benefit distribution calculated with annual wind power data. For further verification, the simulation results of recent three years are included in Table 5.

**Table 5** Monthly benefit distribution of recent three years

Mon	2012		2013		2014	
	Value (\$)	Percentage	Value (\$)	Percentage	Value (\$)	Percentage
1	0	0	0	0	0	0
2	0	0	0	0	0	0
3	15989	2.8	13549	2.4	14765	2.6
4	35695	6.2	36127	6.3	34918	6.1
5	58469	10.2	57386	10.0	56153	9.8
6	77113	13.5	75593	13.2	78074	13.6
7	112395	19.6	117316	20.5	114728	20.0
8	110153	19.2	113068	19.7	112273	19.6
9	76995	13.4	77136	13.5	75343	13.2
10	59531	10.4	57498	10.0	59342	10.3
11	26373	4.6	25368	4.3	26945	4.7
12	531	0.09	347	0.06	417	0.07

It can be seen that strong wind in winter needs most ESS capacity to address the fluctuation issue, and consequently the benefits in winter, i.e. December, January and February, are close to zero. While in summer, much unutilized ESS capacity can participate in power supply for peak load, and the benefits in July are considerable, which are more than 0.11 million dollars. The summer benefits including June, July, and August, are about 53% of total benefits of one whole year. In addition, annual benefits show similar trends and maximum values, as the wind power has annual periodic features. The benefit analysis provides further verification for the presented sizing strategy which takes seasonal variations of wind energy into consideration.

## 7. Conclusion

This paper proposes a novel smoothing control and sizing approach for substation-scale ESS. By considering the seasonal variations in wind energy, the charge and discharge control strategy is presented to achieve extra benefits from power supply for peak load with the spare ESS capacity in mild wind seasons. Based on the proposed control rules, the optimal ESS size can be determined, aiming at minimizing the total investment. The case study with historical wind power data proves that the determined ESS can effectively mitigate wind power fluctuations, also have better economic performance. For future research, since ESS has potential for power supply for peak load, frequency regulation, voltage support, etc, more attention should be paid on the cooperated and optimal operation and control of ESS, which tends to be a multifunctional unit to deal with the problems of the power system. With the increasing capacity, there is a high possibility for ESS to play a significant role in the future power grid.

## 8. Acknowledgement

This work was supported by the National Natural Science Foundation of China under Grant 51307101 and 71401017, in part by the Hong Kong RGC Theme Based Research Scheme under Grant T23-407/13N and T23-701/14N, in part by the Faculty of Engineering and IT Early Career Researcher and Newly Appointed Staff Development Scheme 2016, and in part by funding from the Faculty of Engineering & Information Technologies, The University of Sydney, under the Faculty Research Cluster Program.

## 9. References

- [1] S. Mathew, 'Wind Energy, fundamentals, resource analysis and economics', in *Berlin*, Germany: (Springer- Verlag, 2006)
- [2] A. Sturt, G. Strbac, 'Efficient stochastic scheduling for simulation of wind integrated power systems', *IEEE Trans. Power Syst.*, 2012, 27, 1, pp 323–334
- [3] N. Amutha, B. Kalyan Kuma, 'Effect of modeling of induction generator based wind generating systems on determining CCT', *IEEE Trans. Power Syst.*, 2013, 28, 4, pp 4456–4464

- [4] D.L. Yao, S.S. Choi, K.J. Tseng, *et al.*, 'Determination of short-term power dispatch schedule for a wind farm incorporated with dual-battery energy storage scheme', *IEEE Trans. Sustain. Energy*, 2012, 3, 1, pp74–84
- [5] Q. Li, S.S. Choi, Y. Yuan, *et al.*, 'On the determination of battery energy storage capacity and short-term power dispatch of a wind farm', *IEEE Trans. Sustain. Energy*, 2011, 2, 2, pp 148–158
- [6] K. Meng, Z.Y. Dong, Y. Zheng, *et al.*, 'Optimal allocation of ESS in distribution systems considering wind power uncertainties', *Adv. in Power Syst. Contr. Oper. Manag.*, Hong Kong, 2012.
- [7] Q. Jiang, Y. Gong, and H. Wang, 'A battery energy storage system dual-layer control strategy for mitigating wind farm fluctuations', *IEEE Trans. Power Syst.*, 2013, 28, 3, pp 3263–3273
- [8] A. Damiano, G. Gatto, I. Marongiu, *et al.*, 'Real-time control strategy of energy storage systems for renewable energy sources exploitation', *IEEE Trans. Sustain. Energy*, 2014, 5, 2, pp567–576
- [9] S. Teleke, M.E. Baran, S. Bhattacharya, *et al.*, 'Rule-based control of battery energy storage for dispatching intermittent renewable sources', *IEEE Trans. Sustain. Energy*, 2010, 1, 3, pp 117–124
- [10] T.K.A. Brekken, A. Yokochi, A. von Jouanne, *et al.*, 'Optimal energy storage sizing and control for wind power application', *IEEE Trans. Sustain. Energy*, 2011, 2, 1, pp 69–77
- [11] H.T. Le, S. Santoso, and T.Q. Nguyen, 'Augmenting wind power penetration and grid voltage stability limits using ESS: application design, sizing, and a case study', *IEEE Trans. Power Syst.*, 2012, 27, 1, pp 161–171
- [12] L. Xu, X. Ruan, C. Mao, *et al.*, 'An improved optimal sizing method for wind-solar-battery hybrid power system', *IEEE Trans. Sustain. Energy*, 2013, 4, 3, pp 774–785
- [13] F. Luo, K. Meng, Z.Y. Dong, *et al.*, 'Coordinated operational planning for wind farm with battery energy storage system', *IEEE Trans. Sustain. Energy*, 2015, 6, 1, pp 253–262
- [14] K. Alvehag and L. Söder, 'A reliability model for distribution systems incorporating seasonal variations in severe weather', *IEEE Trans. Power Syst.*, 2011, 26, 2, pp 910–919
- [15] C. Wan, Z. Xu, and P. Pinson, 'Direct interval forecasting of wind power', *IEEE Trans. Power Syst.*, 2013, 28, 4, pp 4877–4878
- [16] J. Barton, and D. Infield, 'Energy storage and its use with intermittent renewable energy', *IEEE Trans. Energy Convers.*, 2004, 19, 2, pp 441–448
- [17] G.L. Soloveichik, 'Battery technologies for large-scale stationary energy storage', *Annual Review of Chemical and Biomolecular Engineering*, 2011, 2, 503–527
- [18] P. Li, H. Banakar, P.K. Keung, *et al.*, 'Macromodel of spatial smoothing in wind farms', *IEEE Trans. Energy Convers.*, 2007, 22, 1, pp 119–128
- [19] K.W. Wee, S.S. Choi, and D.M. Vilathgamuwa, 'Design of a least-cost battery super-capacitor energy storage system for realizing dispatchable wind power', *IEEE Trans. Sustain. Energy*, 2013, 4, 3, pp 786–795
- [20] Y. Xia, S.G. Ghiocel, D. Dotta, *et al.*, 'A simultaneous perturbation approach for solving economic dispatch problems with emission, storage, and network constraints', *IEEE Trans. Smart Grid*, 2013, 4, 4, pp 2356–2363
- [21] Y. Zheng, Z.Y. Dong, F. Luo, *et al.*, 'Optimal allocation of energy storage system for risk mitigation of DISCOs with high renewable penetrations', *IEEE Trans. Power Syst.*, 2014, 29, 1, pp 212–220
- [22] Z. Yang, J. Zhang, M.C.W. Kintner-Meyer, *et al.*, 'Electrochemical energy storage for green grid', *Chemical Reviews*, 2011, 111, 5, pp 3577–3613
- [23] K. C. Divya, and J. Østergaard, 'Battery energy storage technology for power systems—An overview', *Electric Power Systems Research*, 2009, 79, pp 511–520
- [24] F. Bouffard, and F.D. Galiana, 'Stochastic security for operations planning with significant wind power generation', *IEEE Trans. Power Syst.*, 2008, 23, 2, pp 306–316
- [25] M.Y. Suberu, M.W. Mustafa, and N. Bashir, 'Energy storage systems for renewable energy power sector integration and mitigation of intermittency', *Renewable and Sustainable Energy Reviews*, 2014, 35, pp 399–514